Cell Reports, Volume *22*

Supplemental Information

Direct Binding between Pre-S1 and TRP-like Domains in TRPP Channels Mediates Gating and Functional Regulation by PIP2

Wang Zheng, Ruiqi Cai, Laura Hofmann, Vasyl Nesin, Qiaolin Hu, Wentong Long, Mohammad Fatehi, Xiong Liu, Shaimaa Hussein, Tim Kong, Jingru Li, Peter E. Light, Jingfeng Tang, Veit Flockerzi, Leonidas Tsiokas, and Xing-Zhen Chen

The supplemental file includes:

SUPPLEMENTAL FIGURES

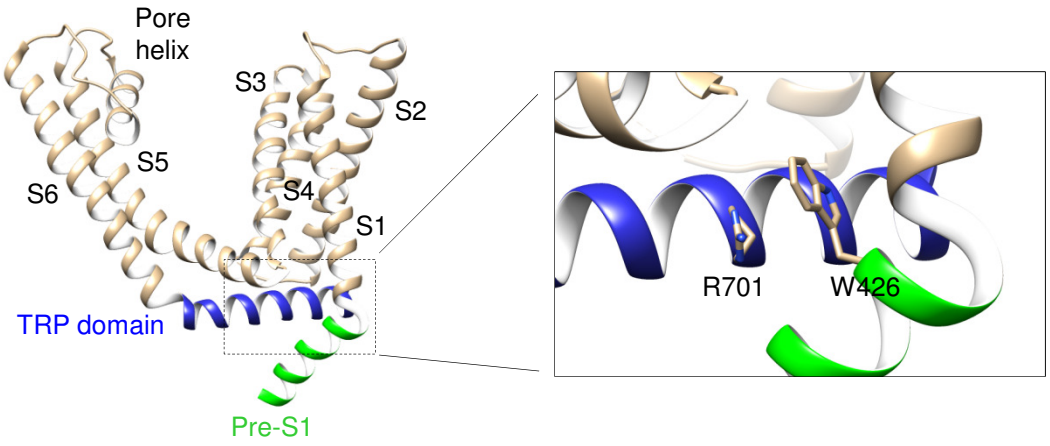

Figure S1. Physical proximity between TRPV1 pre-S1 and TRP domains, related to Figure 1

Ribbon diagram of TRPV1 structure (PDB: 3J5P) showing direct contact between N-terminal pre-S1 (green) and C-terminal TRP helices (blue). The N-terminal fragment before pre-S1 and C-terminal fragment after the TRP domain are not shown**.** The π-cation stacking between W426 and R701 was shown.

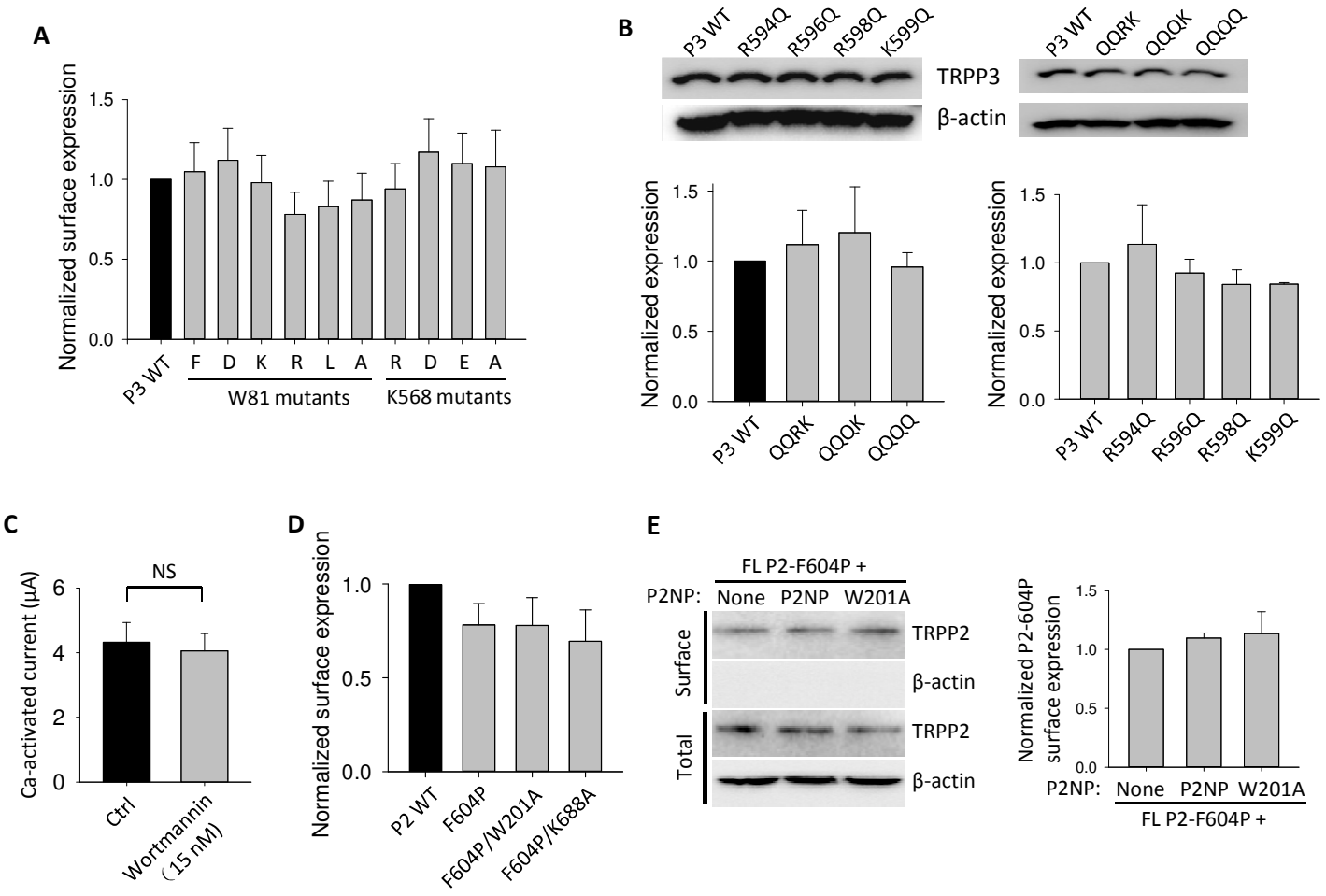

Figure S2. Effects of mutations on TRPP3 or TRPP2 surface expression and effects of 15 nM wortmannin on TRPP3 channel function, related to Figures 1, 2 and 5

(A) Averaged and normalized surface expression of TRPP3 WT, W81 or K568 point mutants from three independent experiments.

(B) *Upper panel*, representative immunoblots of total protein of TRPP3 WT or mutant expressed in oocytes. QQRK, R594Q/R596Q double mutant; QQQK, R594Q/R596Q/R598Q triple mutant; QQQQ, R594Q/R596Q/R598Q/K599Q quadruple mutant. *Lower panels*, data from three independent experiments in *upper panel* were quantified, averaged and normalized.

(C) Averaged Ca-activated currents obtained from TRPP3-expressing oocytes pre-incubated with 15 nM wortmannin or DMSO (Ctrl) for 1 hr before measurements. NS, no significance by t-test.

(D) Averaged and normalized surface expression of TRPP2 WT or indicated mutants from three independent experiments.

(E) *Left panel*, representative immunoblots of the surface biotinylated and total protein of the FL TRPP2 F604P mutant co-expressed with P2NP, P2NP-W201A, or none. β-actin was used as a control. *Right panel*, data from three independent experiments in *left panel* were quantified, averaged and normalized.

Data are presented as mean ± SEM.

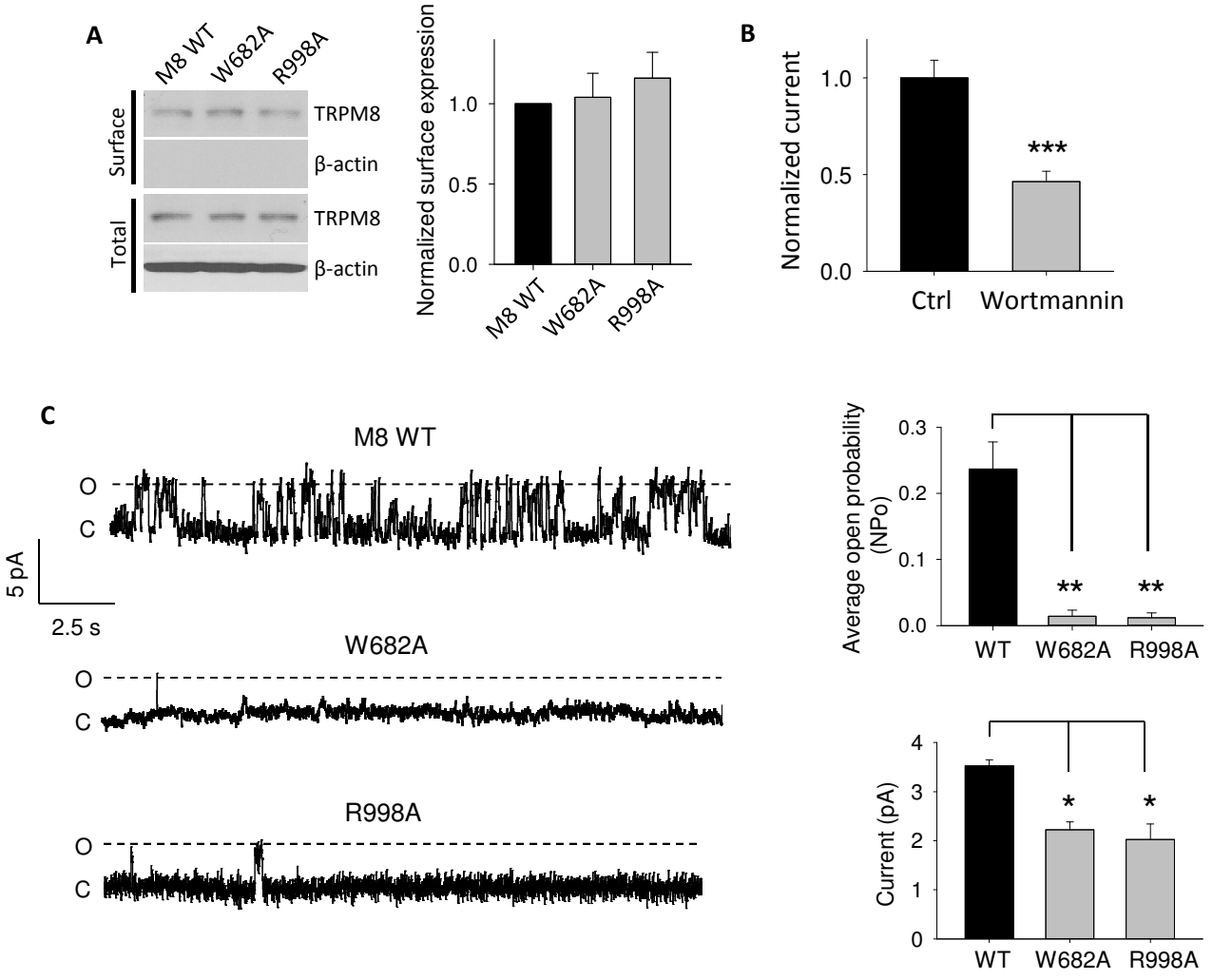

Figure S3. **Surface expression and single-channel currents of WT and mutant TRPM8, related to Figure 4**

(A) *Left panel*, representative immunoblots of the surface biotinylated and total protein of TRPM8 WT or indicated mutants expressed in oocytes. β-actin was used as a control. *Right panel*, data from three independent experiments in *left panel* were quantified, averaged and normalized.

(B) Averaged and normalized 0.5 mM menthol-induced currents obtained from TRPM8-expressing oocytes pre-incubated with 10 μM wortmannin or DMSO (Ctrl) for 1 hr before measurements.

(C) *Left panel*, representative single-channel traces recorded at +100 mV in HEK293 cells expressing TRPM8 WT (n = 5), W682A (n = 5) or R998A (n = 4) mutant under the cell-attached configuration. 'C' and 'O' indicate the closed and open states, respectively. Measurements were performed as previously (Zheng et al., 2017). *Right panels*, averaged channel open probabilities and current amplitudes obtained from single-channel recordings each of around 20-s duration.

Data are presented as mean ± SEM. Statistical analyses were performed with t-test. *$p < 0.05$; **$p < 0.01$; ***$p < 0.001$.

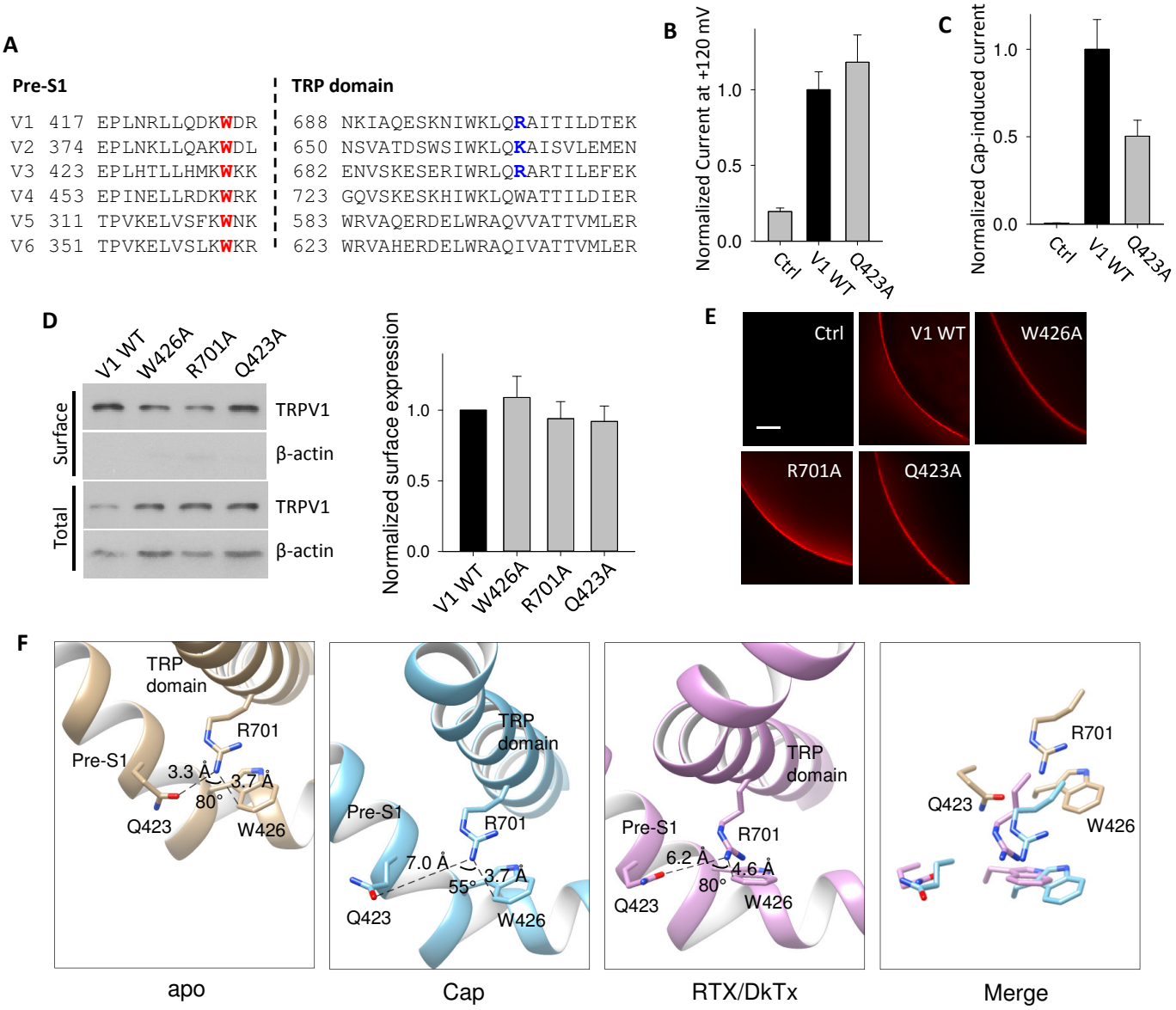

Figure S4. Effects of mutations on the expression, function and N-C interaction of TRPV1, related to Figure 4

(A) Amino acid alignment of human TRPVs pre-S1 and TRP domains. Conserved aromatic W and cationic R/K (except TRPV4-6) are indicated in red and blue, respectively.

(B) Averaged and normalized currents at +120 mV under the same experimental conditions as Figure 4G *left panel* from oocytes expressing TRPV1 WT or Q423A mutant. Ctrl, H_2O-injected oocytes.

(C) Averaged and normalized capsaicin-induced currents under the same experimental conditions as Figure 4H *left panel* from oocytes expressing TRPV1 WT or Q423A mutant. Ctrl, H_2O-injected oocytes.

(D) *Left panel*, representative immunoblots of surface biotinylated and total protein of TRPV1 WT or mutant expressed in oocytes. β-actin was used as a control. *Right panel*, data from three independent experiments in *left panel* were quantified, averaged and normalized.

(E) Representative whole-mount immunofluorescence showing surface expression of TRPV1 WT or mutant expressed in an oocyte. Ctrl, H_2O-injected oocyte. *Scale bar*, 50 μm.

(F) Relative position of TRPV1 R701 to Q423 and W426 in the apo state (PDB 3J5P), the activated state in the presence of capsaicin (Cap, PDB 3J5R), and the combined presence of vanilloid agonist resiniferatoxin (RTX) and spider double-knot toxin (DkTx) (PDB 3J5Q). *Right panel*, merge of the three residues at the different states.

Data are presented as mean ± SEM.

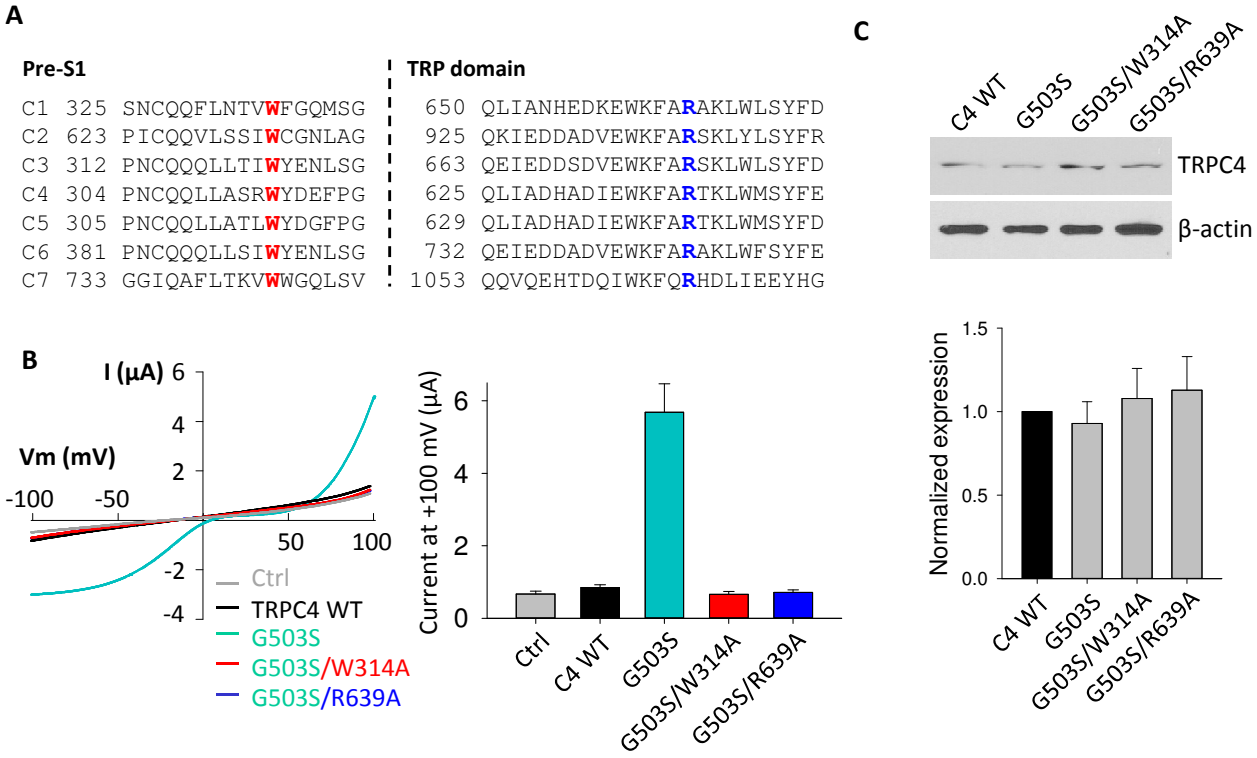

Figure S5. Roles of the mouse TRPC4 residues W314 (pre-S1) and R639 (TRP domain) in the channel function, related to Figure 4

(A) Amino acid alignment of human TRPCs pre-S1 and TRP domains. Human *TRPC2* is a pseudogene and mouse TRPC2 was used instead. Conserved aromatic W and cationic R are indicated in red and blue, respectively.

(B) *Left panel*, representative I-V curves obtained from oocytes expressing mouse WT or a mutant TRPC4β, as indicated, in the presence of a Na^+-containing solution. Ctrl, H_2O-injected oocytes. *Right panel*, averaged currents at +100 mV under the same experimental conditions as in *left panel*.

(C) *Upper panel*, representative immunoblots of total protein of TRPC4β WT or mutant expressed in oocytes. *Lower panel*, data from three independent experiments in *upper panel* were quantified, averaged and normalized.

Data are presented as mean ± SEM.

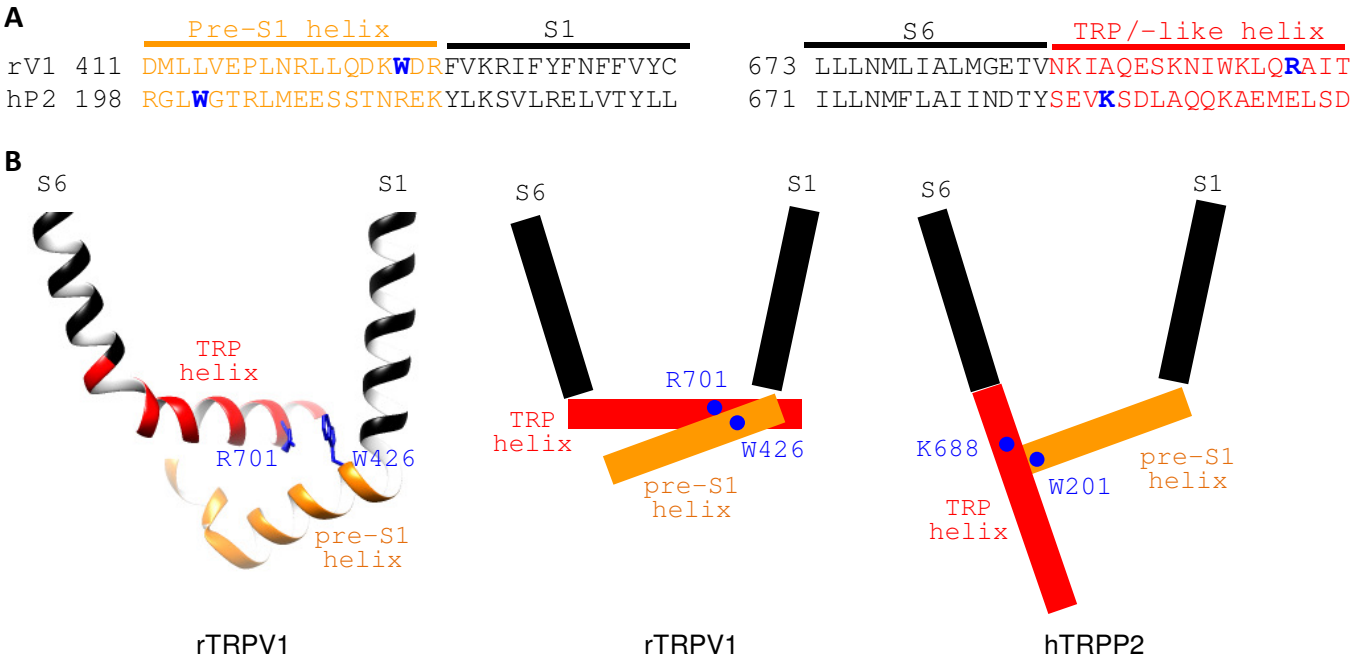

Figure S6. Comparison of the N-C interaction in TRPV1 and TRPP2, related to Figures 2 and 4
(A) Sequence alignment of rat TRPV1 (rV1) and human TRPP2 (hP2) showing different positions of the tryptophan residue (blue) in the pre-S1 helix and the cationic residue (blue) in the TRP/TRP-like helix.
(B) *Left panel*, ribbon diagram of TRPV1 structure (PDB: 3J5P) showing direct contact between the pre-S1 helix (orange) and TRP helix (red). W426 and R701 residues are shown. *Central panel*, schematic illustration (with a horizontal TRP helix) showing the W426-R701 interaction in TRPV1. *Right panel*, schematic illustration (with TRP-like helix parallel to S6) showing the W201-K688 interaction in TRPP2.